

Measuring Coronal Magnetic Fields by Pulsar Faraday Rotation

Yoshiki Sofue

SKA Con. on Cosmic Magnetism

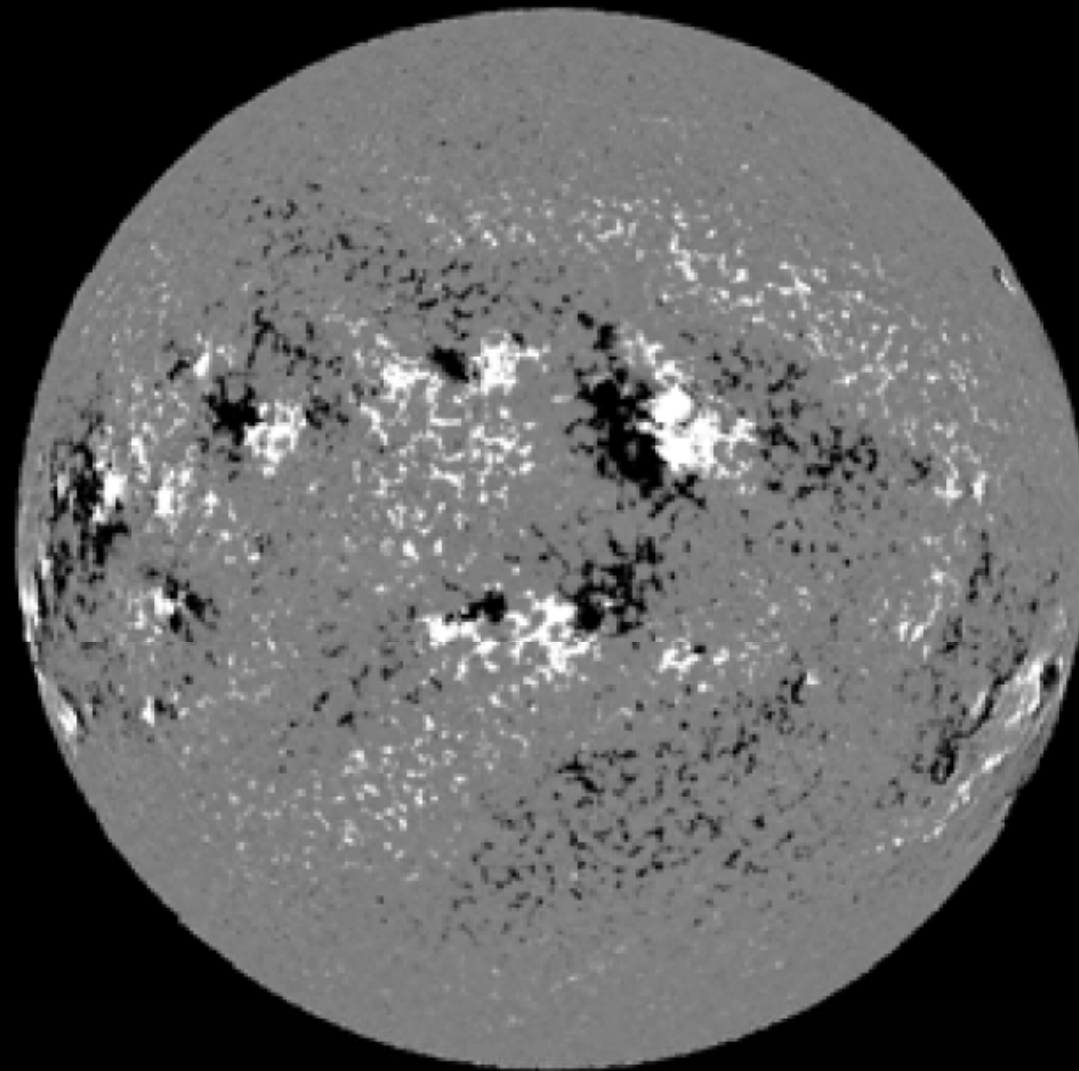
2013 Sep 13-14 @Mizusawa



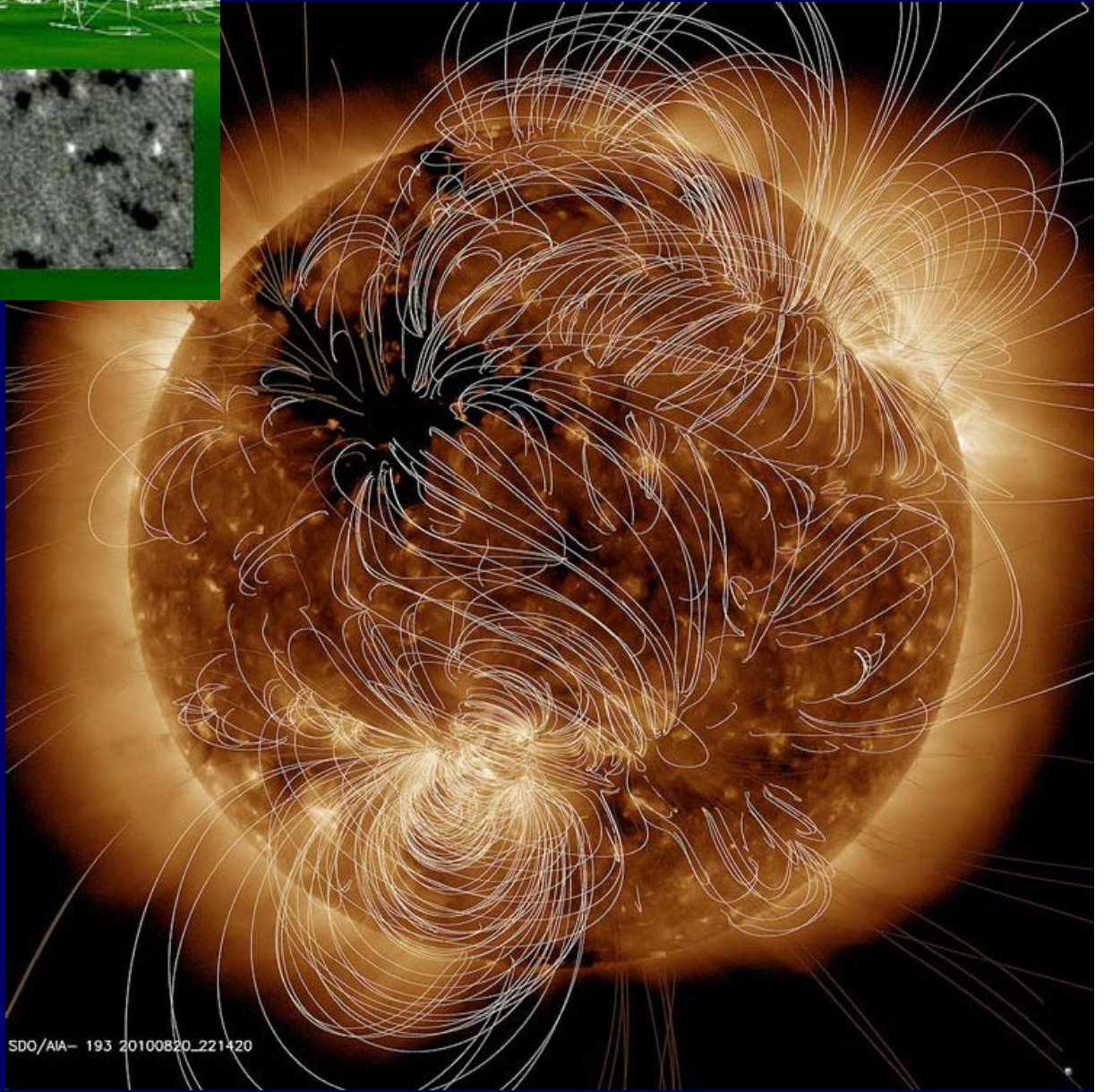
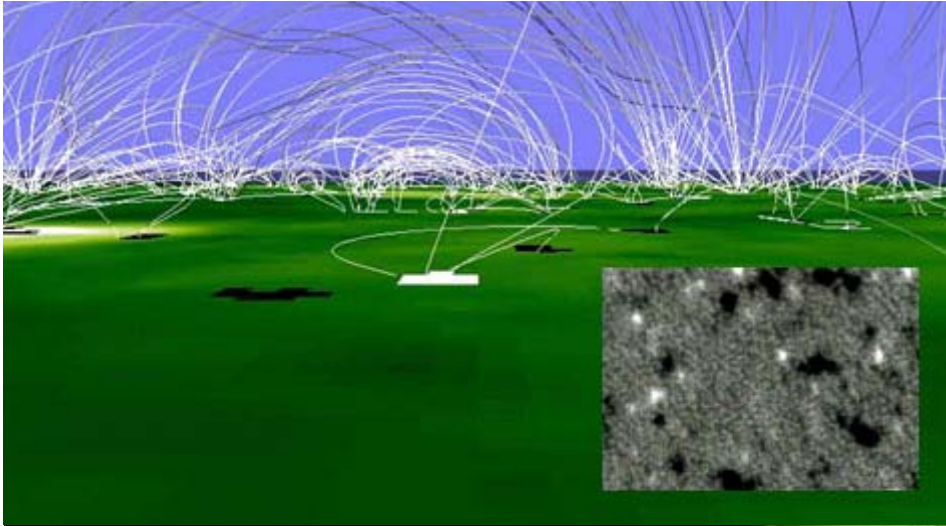
I.
Solar Magnetic Fields

Magnetic map of the Sun

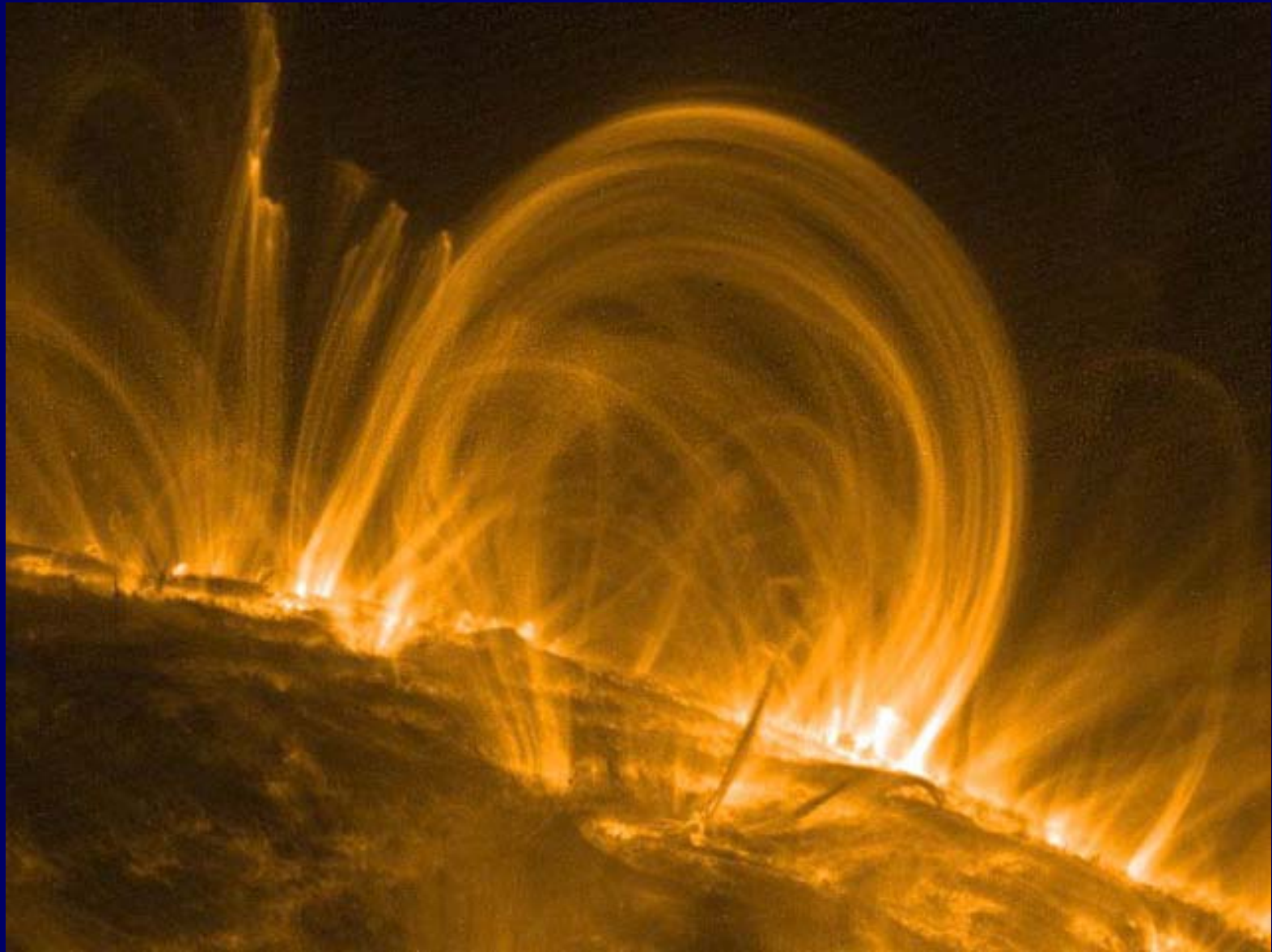
Solar maximum dominated by global dynamo

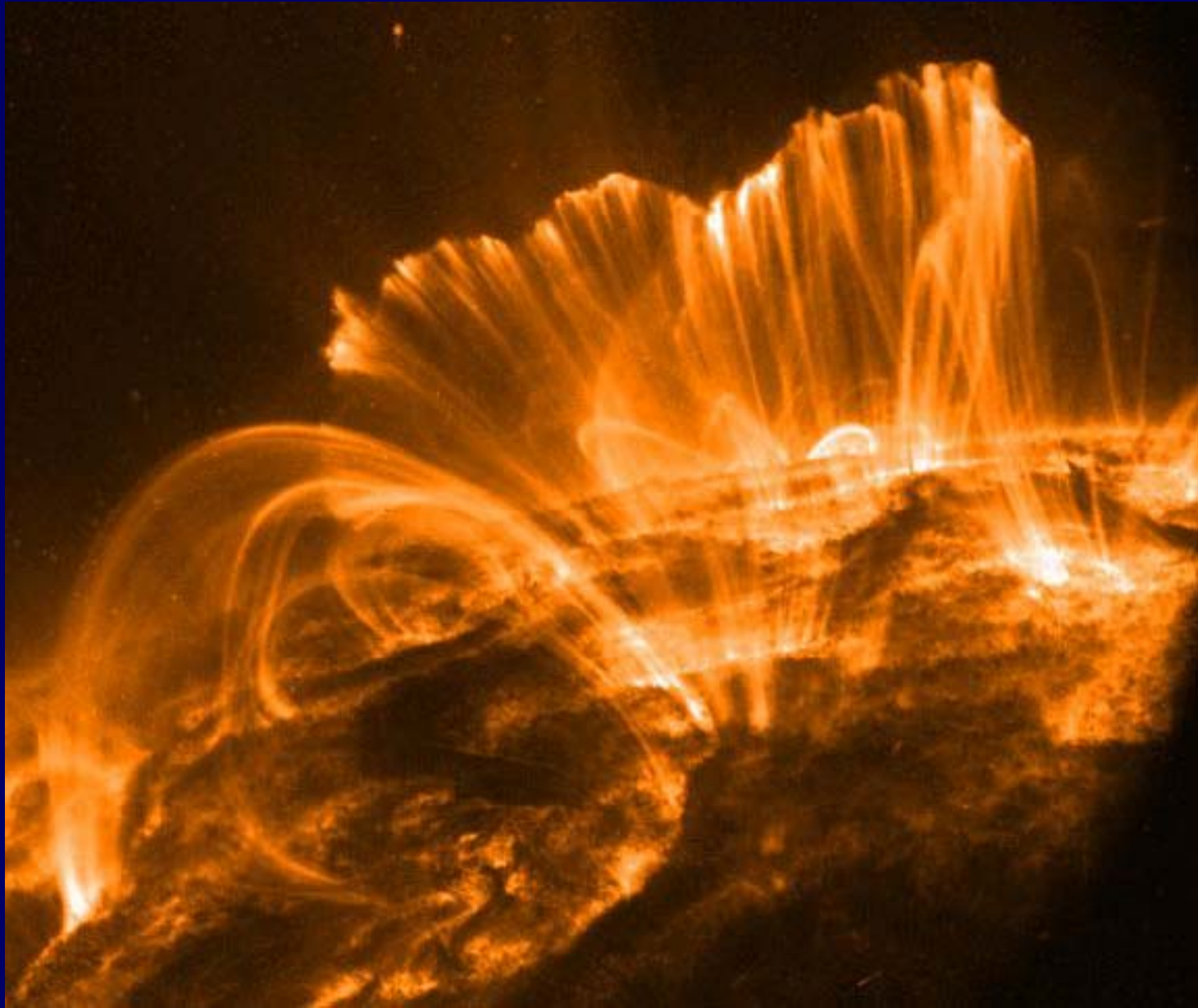


Kitt Peak magnetogram



SDO/AIA- 193 20100820_221420





But !

Few direct measurement of
magnetic fields.

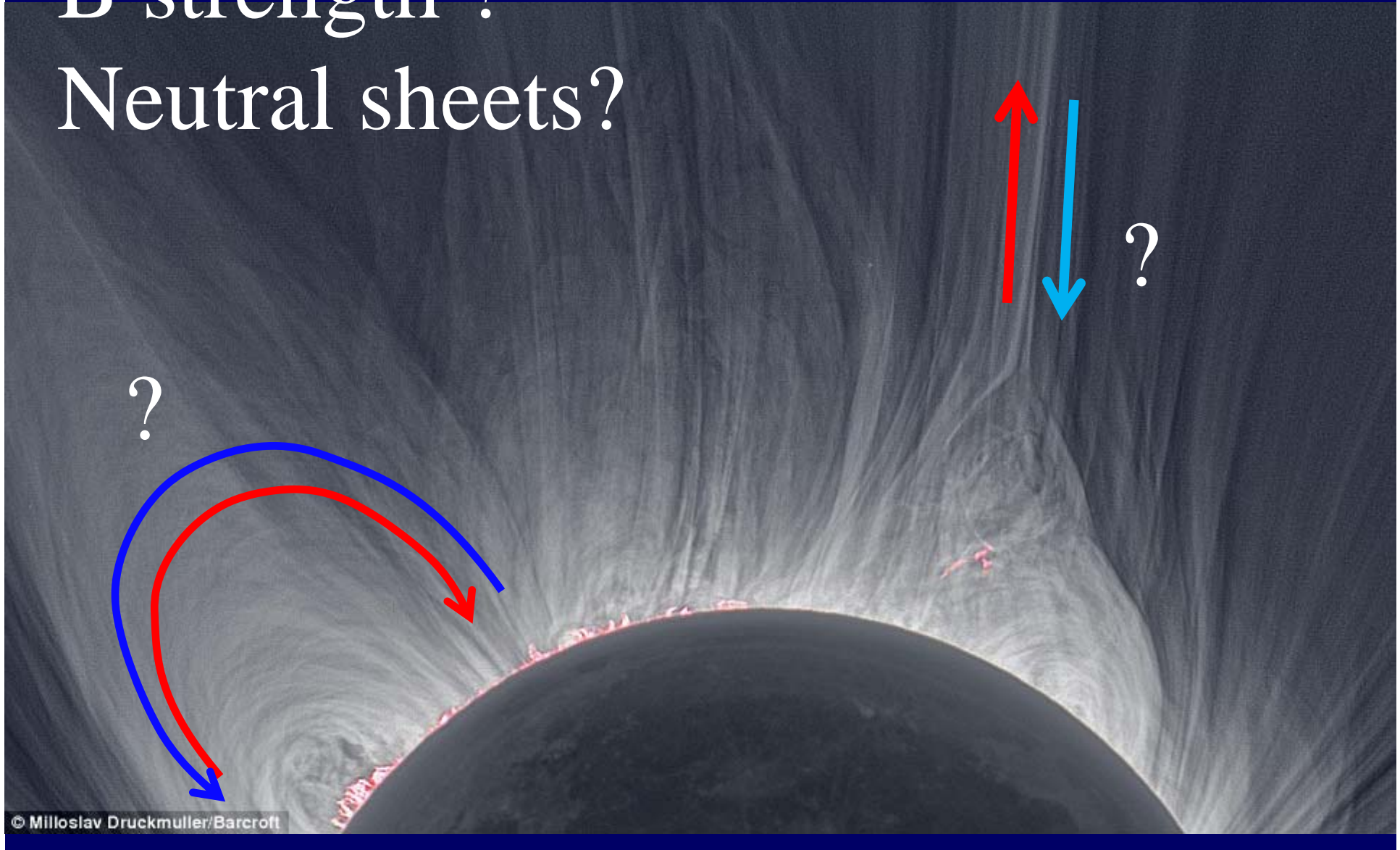



II. Coronal Magnetic Fields

B direction ?

B strength ?

Neutral sheets?

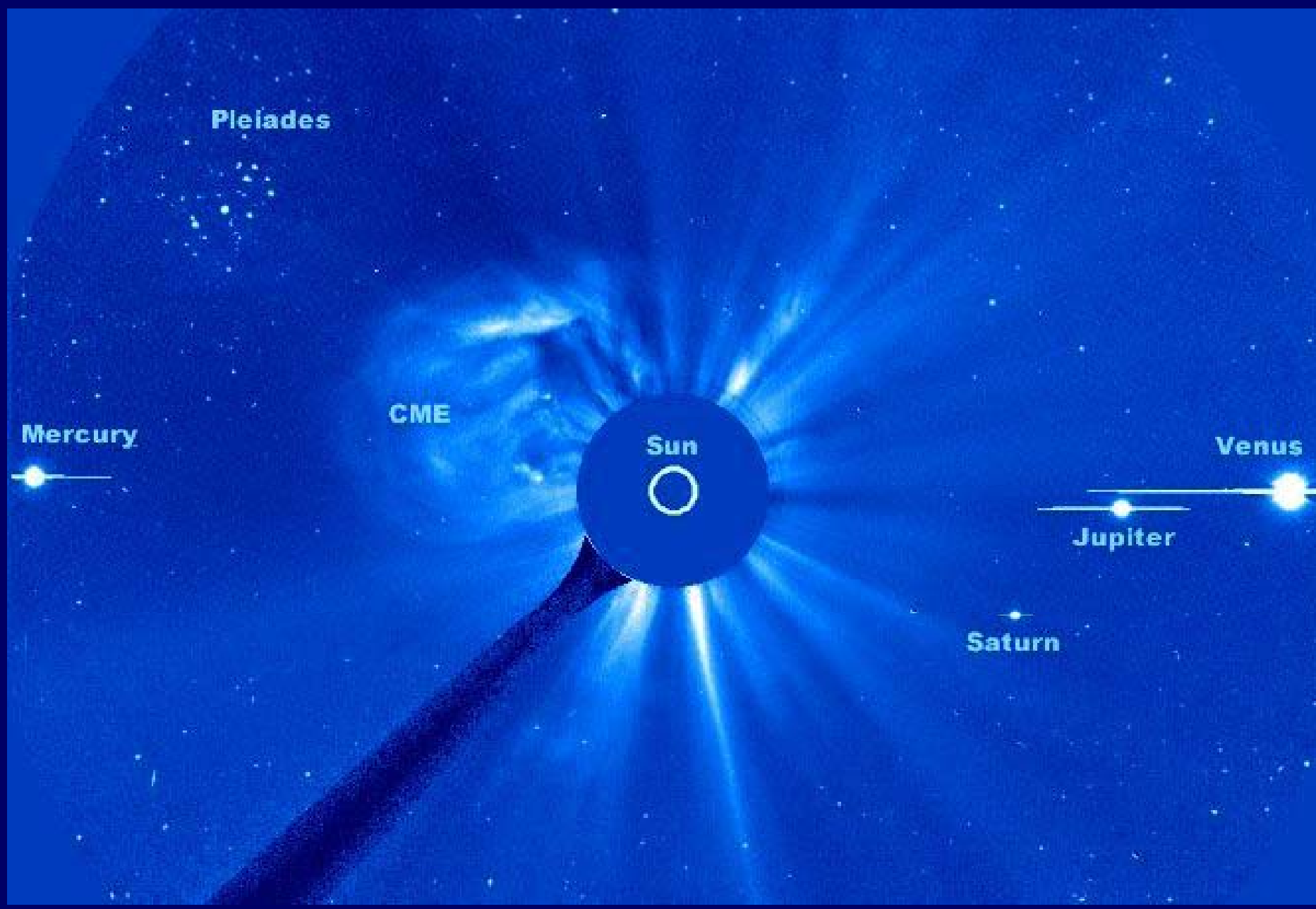


A dark, spherical object, possibly a planet or a black hole, is centered in the frame. It is surrounded by a complex, glowing aura of light rays and energy fields. The rays emanate from the sphere, creating a starburst effect. The background is a dark, deep blue or black, with some faint, wispy light patterns. The overall image has a high-contrast, ethereal quality.

© Miloslav Druckmüller/Barcroft



Miloslav Druckmüller
Institute of Mathematics, Faculty of
Mechanical Engineering
Brno University of Technology, Czech
Republic



Pleiades

Mercury

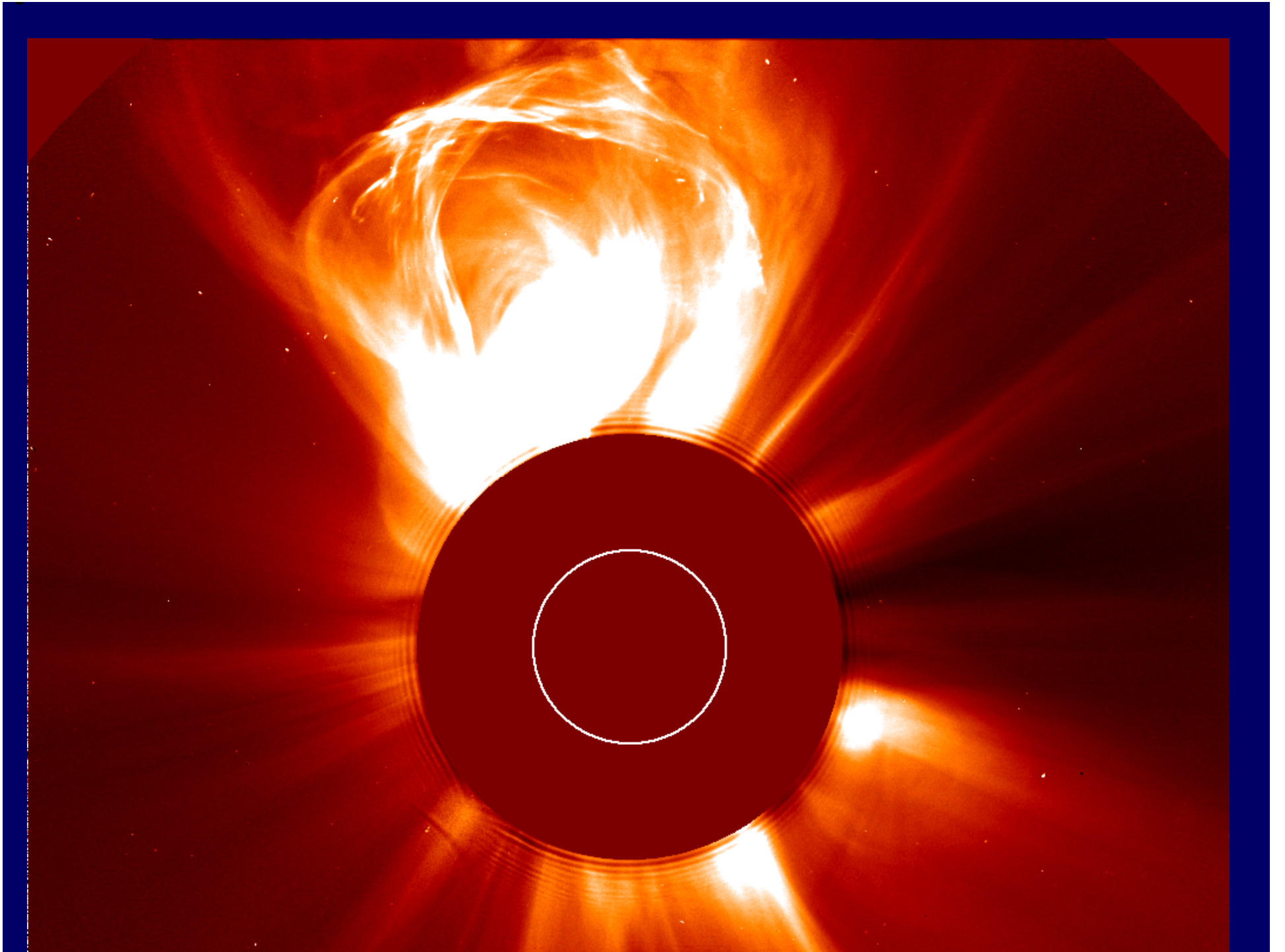
CME

Sun

Venus

Jupiter

Saturn



But !

Few direct measurement of
magnetic field.



III. Current Measurements

Kim+2012

THE ASTROPHYSICAL JOURNAL, 746:118 (8pp), 2012 February 20

KIM ET AL.

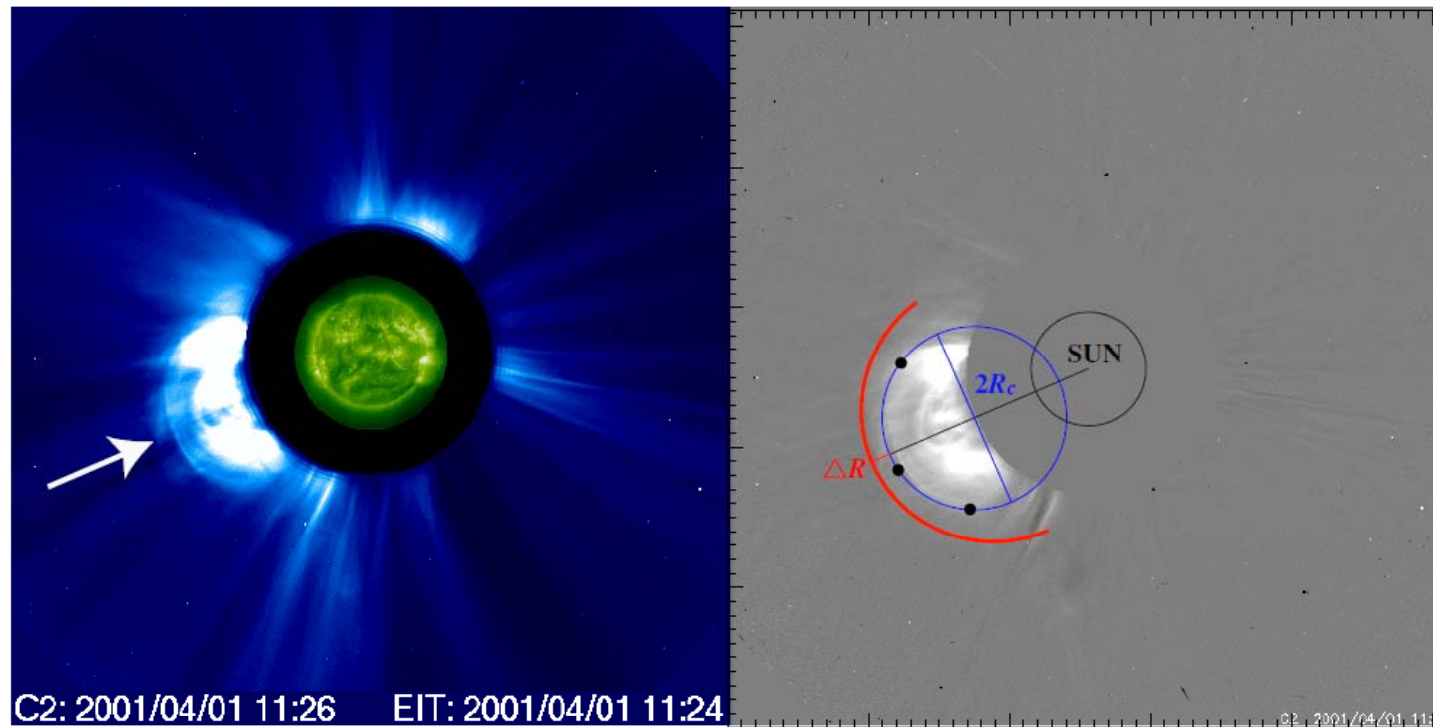


Figure 1. Left panel shows a *SOHO*/LASCO image of the 2001 April 1 CME at 11:26 UT showing the diffuse structure ahead of the CME flux rope (the sharp feature). The arrow indicates the shock nose. The right panel shows the running difference image of the event. The radial black line marks the central P.A. of the shock nose, and the blue circle indicates the CME as an obstacle. The red lines indicate the shock front and standoff distance, ΔR .

Information about Very Fast ($\geq 1000 \text{ km s}^{-1}$) Limb CMEs that Show Clear Shock Structures from 1997 to 2003

No.	CME Date/Time	Type II ^a Time	Shock Position		Shock Parameter			Mach No.		V_A (km s^{-1})		B (mG)	
			P.A. ($^\circ$)	Height (R_s)	$\Delta R/R_c$	ρ_d/ρ_u	V_{SH} (km s^{-1})	$M_{\Delta R}$	M_ρ	$V_{A\Delta R}$	$V_{A\rho}$	$B_{\Delta R}$	B_ρ
1	1997 Nov 14 10:14:03	No	70	3.33	0.78	1.35	862	1.49	1.63	580	527	101	92
	1997 Nov 14 10:52:30		67	6.19	0.35	1.12	988	2.09	1.53	471	647	27	37
2	1999 Jul 25 13:31:21	13:21 M	301	3.08	0.27	1.30	1259	2.51	1.61	501	780	105	163
	1999 Jul 25 13:54:05		301	5.55	0.38	1.22	1370	2.00	1.58	684	869	46	58
	1999 Jul 25 14:18:05		301	8.50	0.53	1.08	1546	1.71	1.51	902	1025	34	38
	1999 Jul 25 14:42:05		301	11.7	0.54	1.05	1400	1.70	1.49	825	937	21	24
3	2000 Apr 4 16:43:01	15:31 M	325	11.46	0.55	1.01	1279	1.68	1.48	761	867	20	23
	2000 Apr 4 17:18:06	15:45 D	326	15.33	0.34	1.00	1049	2.12	1.47	494	711	10	14
4	2000 May 4 11:42:05	11:06 M	226	7.92	0.61	1.14	705	1.62	1.53	435	459	18	19
	2000 May 4 12:42:05	11:10 D	226	12.64	0.20	1.07	1142	3.20	1.51	356	758	8	18
5	2000 May 5 16:18:05	16:35 D	213	6.35	0.37	1.17	1308	2.03	1.55	643	843	35	46
	2000 May 5 16:42:06		214	9.06	0.33	1.12	1299	2.16	1.53	601	851	21	29
6	2000 Jun 15 20:26:06	19:43 M	306	6.06	0.31	1.08	761	2.25	1.51	338	504	20	29
	2000 Jun 15 20:42:05	19:52 D	307	7.11	0.33	1.07	1030	2.17	1.51	473	683	22	32
	2000 Jun 15 21:18:05		307	10.31	0.25	1.06	947	2.59	1.50	365	632	11	19
	2000 Jun 15 21:42:05		308	12.27	0.19	1.04	889	3.43	1.49	258	596	6	15
7	2001 Apr 1 11:26:06	No	116	4.21	0.27	1.33	1197	2.45	1.62	488	737	52	79
	2001 Apr 1 11:50:07		117	6.69	0.24	1.12	1318	2.69	1.53	490	861	25	44
8	2001 Dec 28 20:30:05	19:59 M	151	5.98	0.33	1.19	2132	2.17	1.56	981	1366	58	81
	2001 Dec 28 21:18:32	20:35 D	152	14.89	0.25	1.10	2067	2.62	1.52	788	1360	16	27
9	2002 Jan 14 06:05:05	06:08 M	220	4.82	0.25	1.91	1461	2.66	1.90	549	768	46	64
	2002 Jan 14 06:30:05	06:25 D	220	7.78	0.20	1.33	1762	3.19	1.63	551	1083	23	45

Ramesh+2010

RAMESH, KATHIRAVAN, & SASTRY

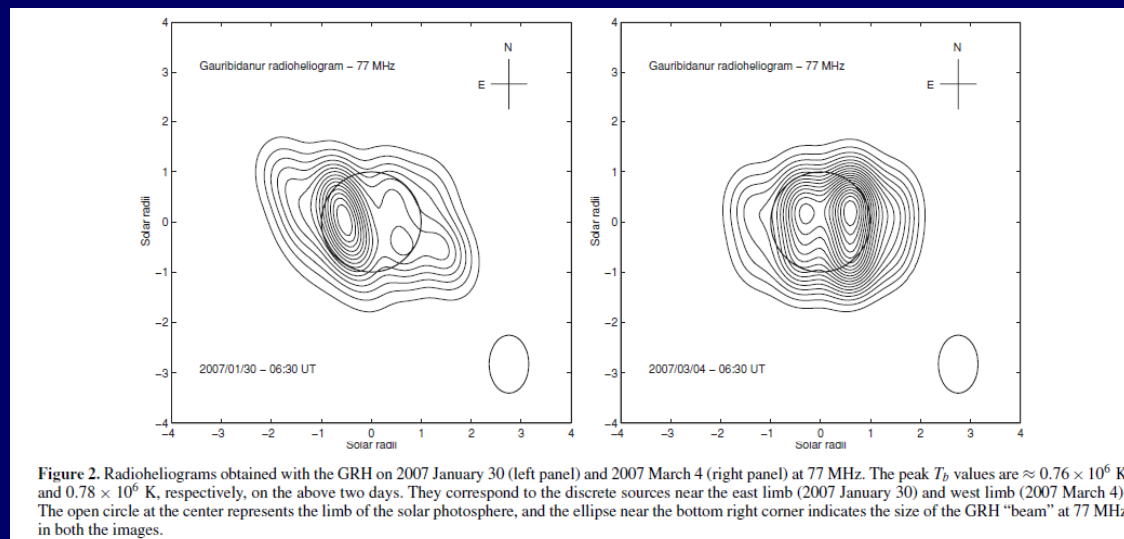
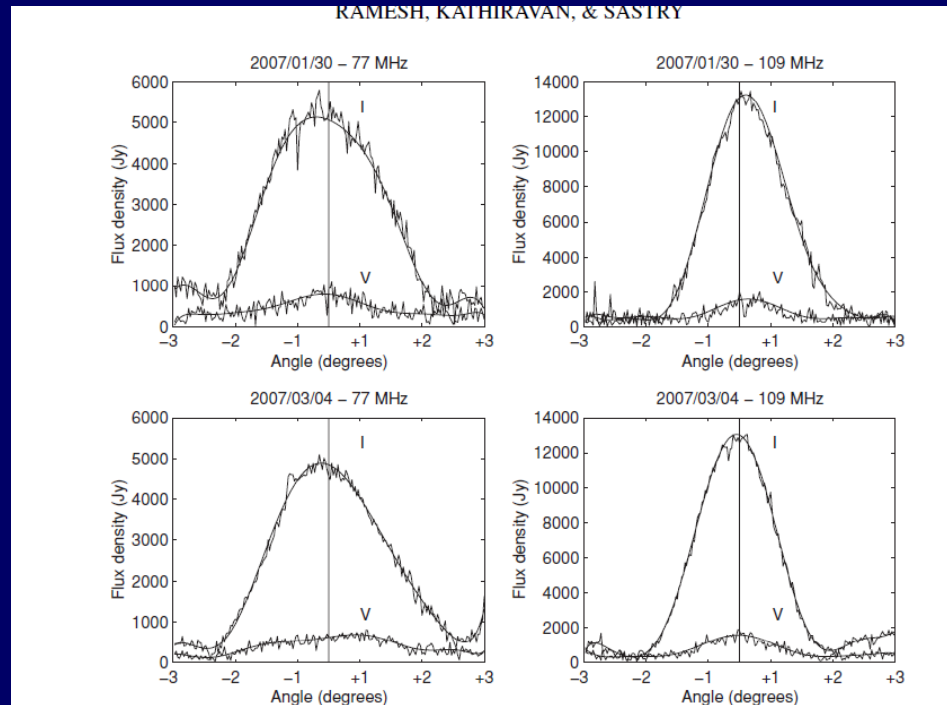
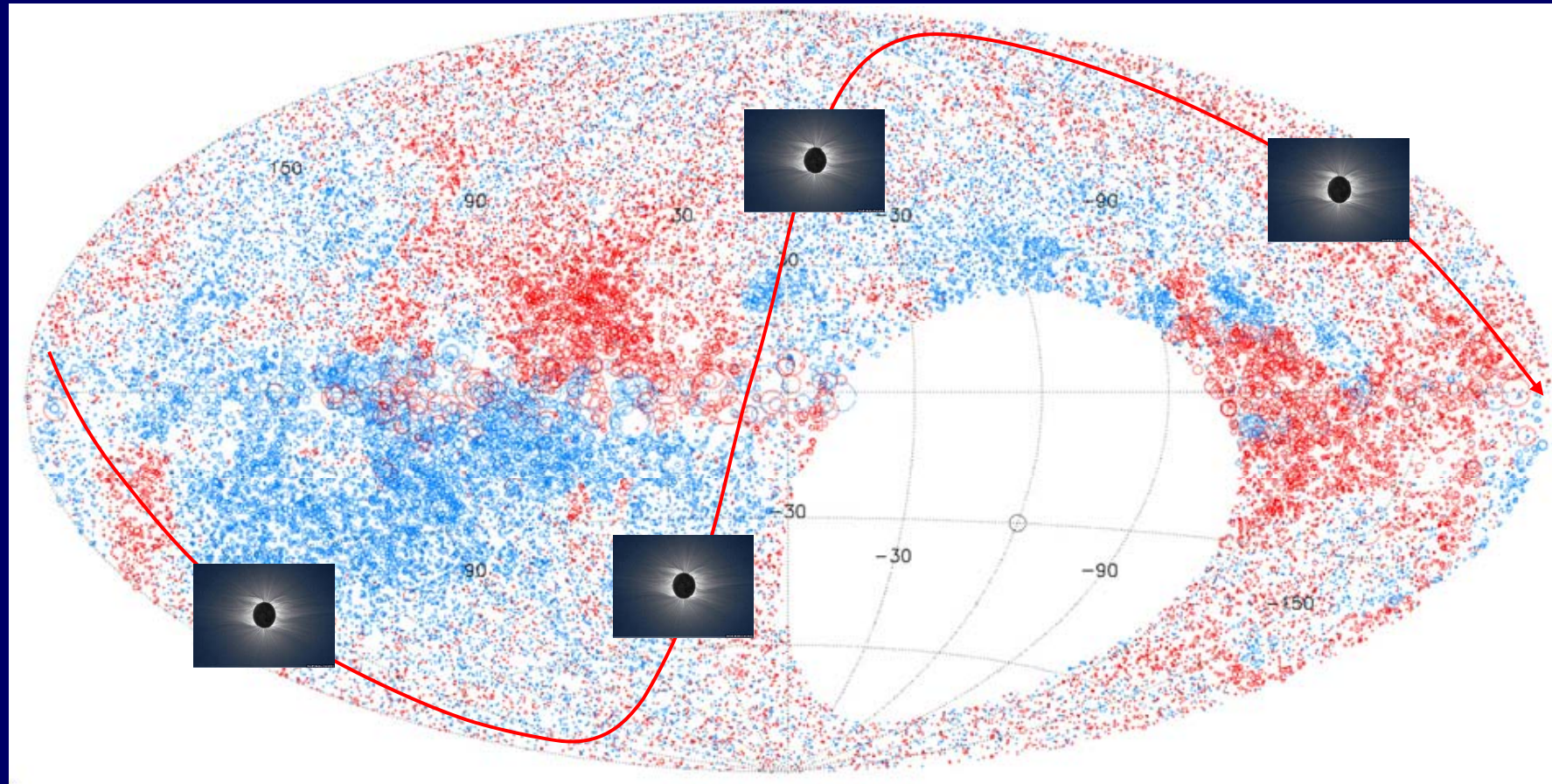


Figure 2. Radioheliograms obtained with the GRH on 2007 January 30 (left panel) and 2007 March 4 (right panel) at 77 MHz. The peak T_b values are $\approx 0.76 \times 10^6$ K and 0.78×10^6 K, respectively, on the above two days. They correspond to the discrete sources near the east limb (2007 January 30) and west limb (2007 March 4). The open circle at the center represents the limb of the solar photosphere, and the ellipse near the bottom right corner indicates the size of the GRH "beam" at 77 MHz in both the images.

Table 1
Details of Gauribidanur Radio Polarimeter and Heliograph Observations

Parameter	2007 January 30	2007 March 4
Polarimeter observations		
109 MHz		
Stokes I flux	$13263 \pm 100 Jy$	$13052 \pm 100 Jy$
Stokes V flux	$1421 \pm 100 Jy$	$1579 \pm 100 Jy$
dcp	$10\% \pm 2\%$	$12\% \pm 2\%$
77 MHz		
Stokes I flux	$5133 \pm 150 Jy$	$4875 \pm 150 Jy$
Stokes V flux	$800 \pm 150 Jy$	$687 \pm 150 Jy$
dcp	$15\% \pm 5\%$	$14\% \pm 5\%$
Spectral index (β)–Stokes I	2.7 ± 0.3	2.8 ± 0.5
Spectral index (β)–Stokes V	1.7 ± 0.3	2.4 ± 0.5
GRH observations		
77 MHz		
Integrated flux	$5342 \pm 200 Jy$	$5643 \pm 200 Jy$
Peak T_b	$0.76 \times 10^6 K$	$0.78 \times 10^6 K$
Magnetic field		
109 MHz ($r \approx 1.5 R_\odot$)	$6 \pm 2 G$	$6 \pm 2 G$
77 MHz ($r \approx 1.7 R_\odot$)	$5 \pm 1 G$	$5 \pm 1 G$

Use SKA for, not only Tau A, but also the Faraday sky

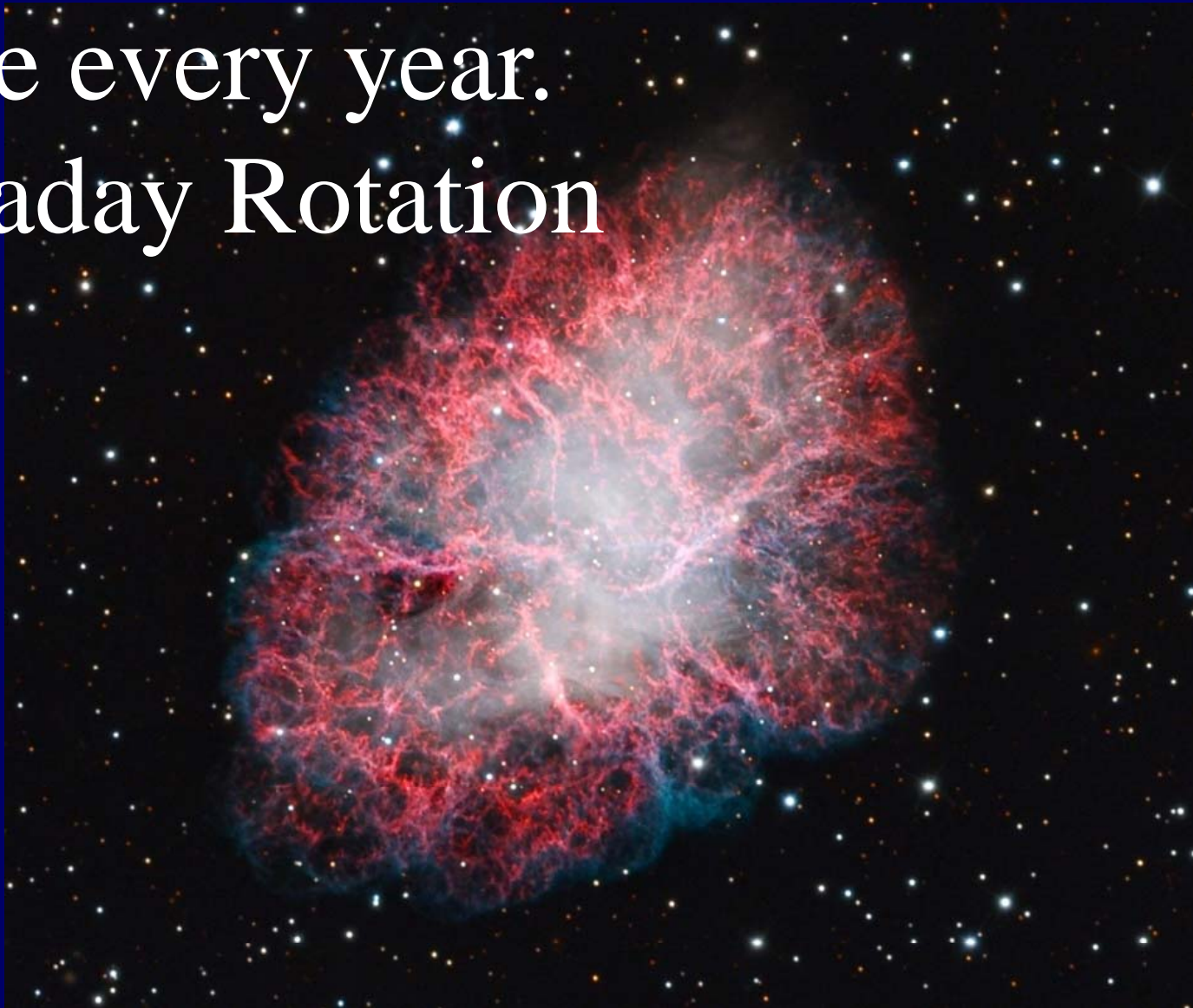


(Taylor 2009)

Coronal Occultation of Tau A

June every year.

Faraday Rotation



Sofue et al 1976 Sol. Phys.

**CORONAL FARADAY ROTATION OF THE CRAB NEBULA,
1971–1975**

Y. SOFUE* and K. KAWABATA

Department of Physics, Nagoya University, Nagoya, Japan

and

F. TAKAHASHI and N. KAWAJIRI

Kashima Station, Radio Research Laboratories, Kashima, Japan

(Received 17 June; in revised form 13 September, 1976)

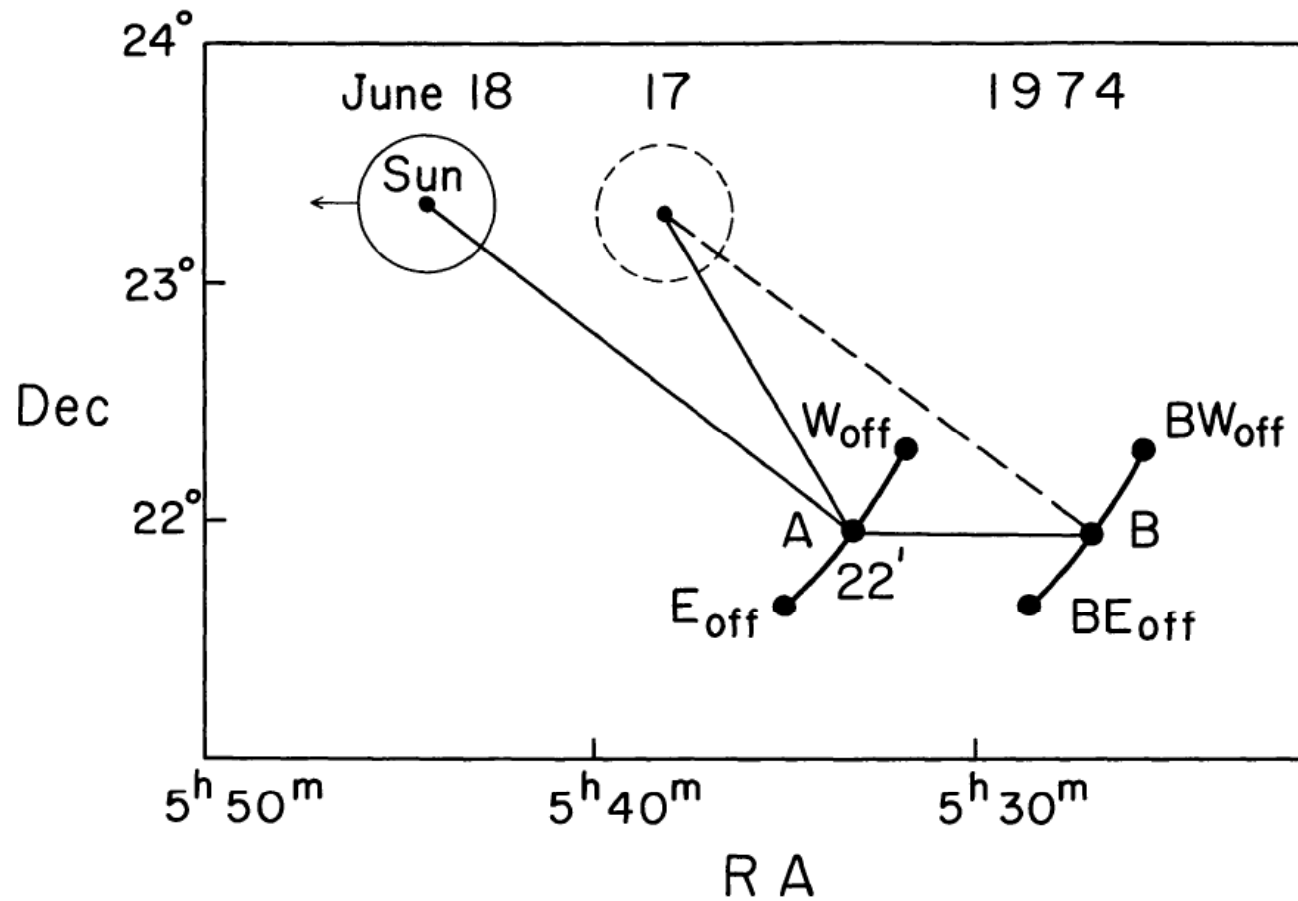
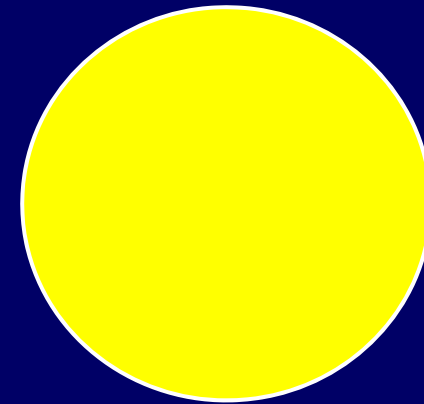
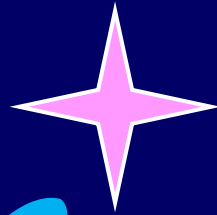


Fig. 1. Relative positions of Tau A (Point A) and the Sun on June 18 and 'off positions' (E_{off} and W_{off}), at

1-1000 x few % Jy



20,000 Jy



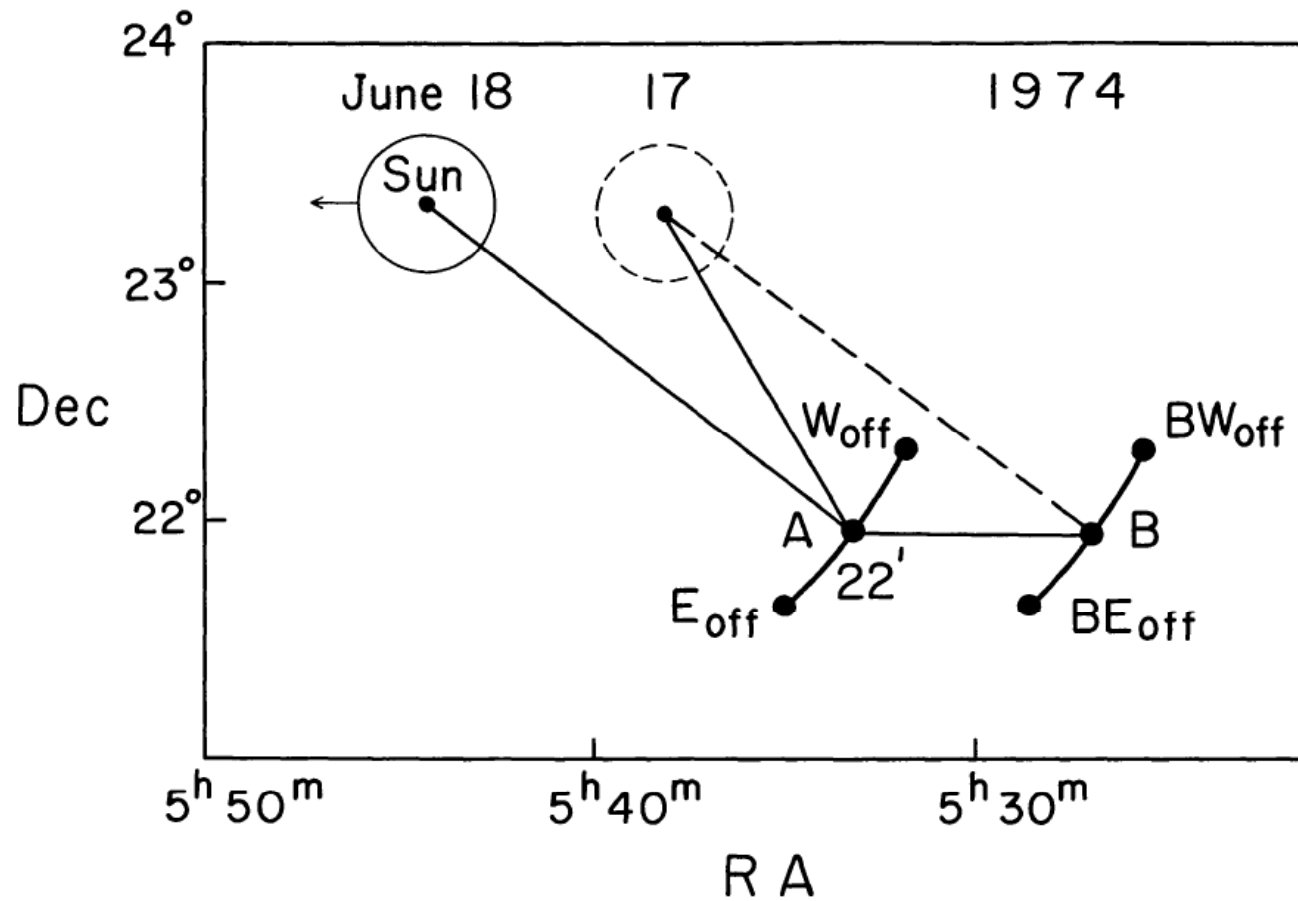
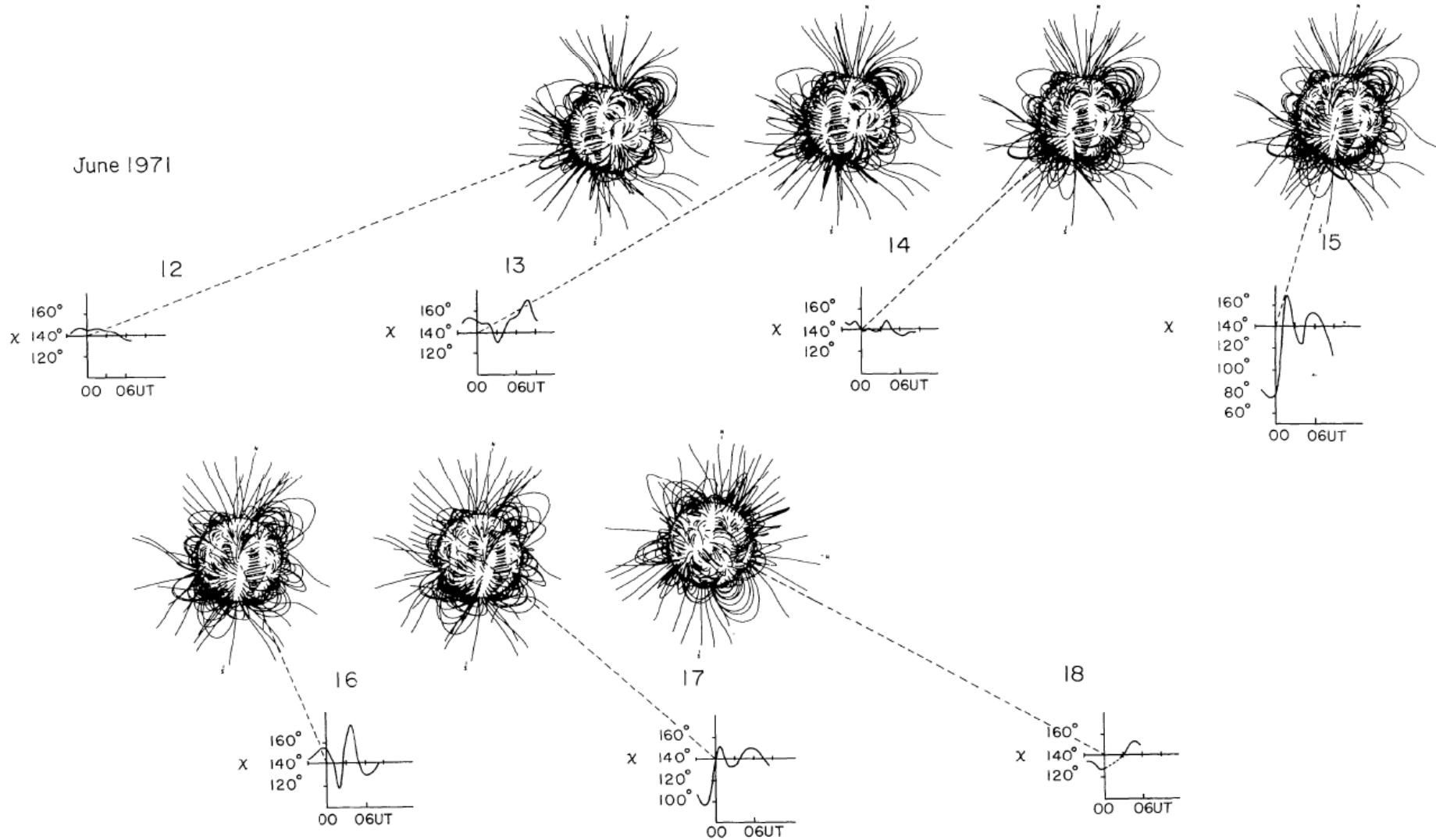
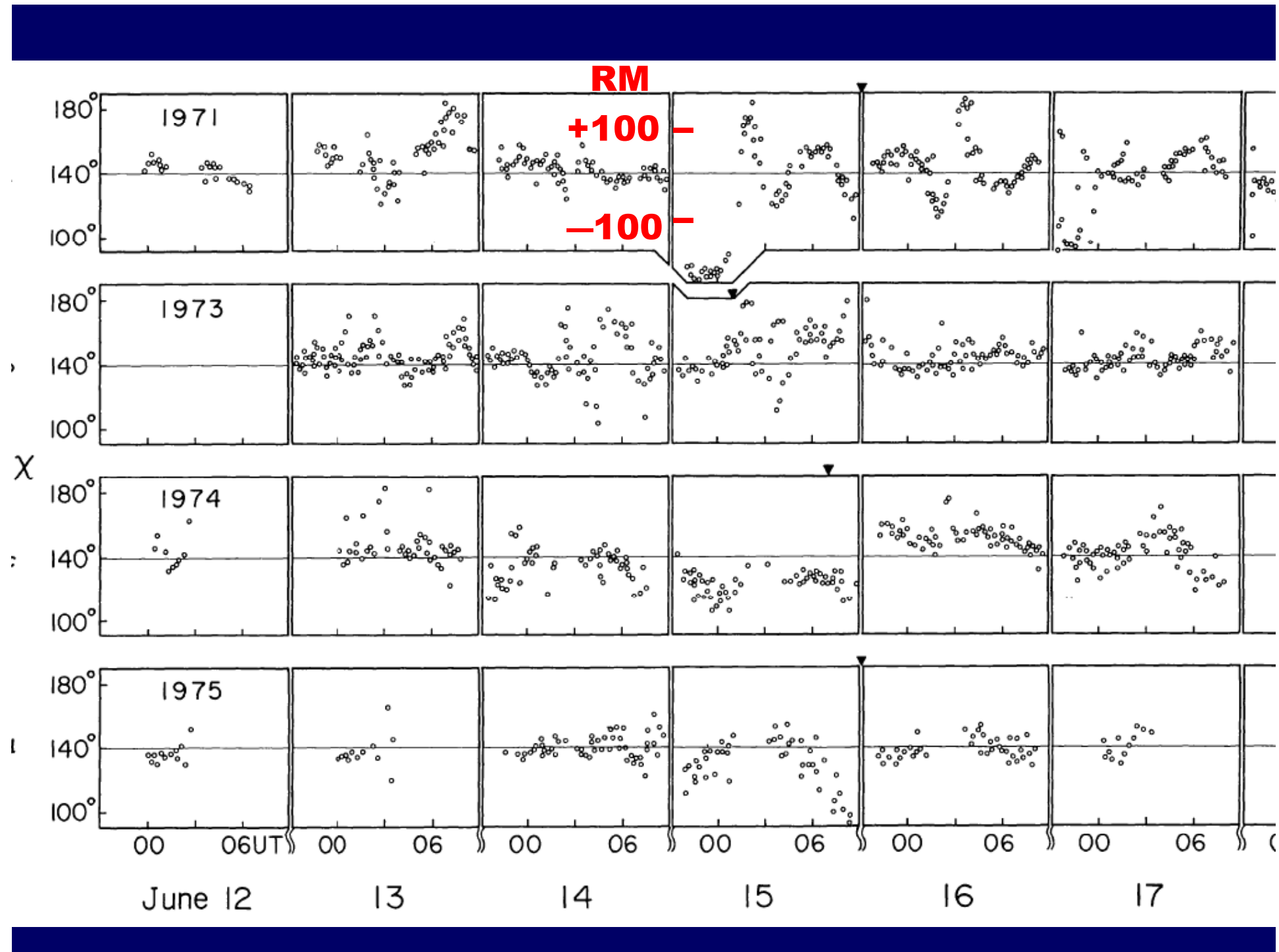


Fig. 1. Relative positions of Tau A (Point A) and the Sun on June 18 and 'off positions' (E_{off} and W_{off}), at

June 1971





$$RM = 0.81 \int N_e [\text{cm}^{-3}] B_{//} [\mu\text{G}] ds [\text{pc}]$$

$$= 1.82 \times 10^{-2} \int N_e [\text{cm}^{-3}] B_{//} [\text{G}] ds / R_{\odot} \quad [\text{rad m}^{-2}]$$

$$N_e \simeq 1.5 \times 10^6 \left(\frac{R}{R_{\odot}} \right)^{-2.5} \quad [\text{cm}^{-3}]$$

$$B \simeq 1 \left(\frac{R}{R_{\odot}} \right)^{-2} \quad [\text{G}]$$

At $R = 1R_{\odot}$, $s = 1R_{\odot}$,

$$N_e \simeq 1.5 \times 10^6 \quad [\text{cm}^{-3}]$$

$$B \simeq 1 \quad [\text{G}]$$

$$RM = 1.82 \times 10^{-2} \times 1.5 \times 10^6 \times 1$$

$$\sim 3 \times 10^4 \quad [\text{rad m}^{-2}]$$

Quiet corona model

At 7 R_o

$$B_{\text{Ne}} = 400 \text{ G cm}^{-3}$$

Across streamer 1971–1973

$$RM = 100\text{--}150 \text{ rad m}^{-2}$$

$$B_{\text{Ne}} = 5000\text{--}8000 \text{ G cm}^{-3}$$

Across streamer 1974–1975

$$RM = 120\text{--}150 \text{ rad m}^{-2}$$

$$B_{\text{Ne}} = 2000\text{--}3500 \text{ G cm}^{-3}$$



IV.
Pulsar Faraday Rotation

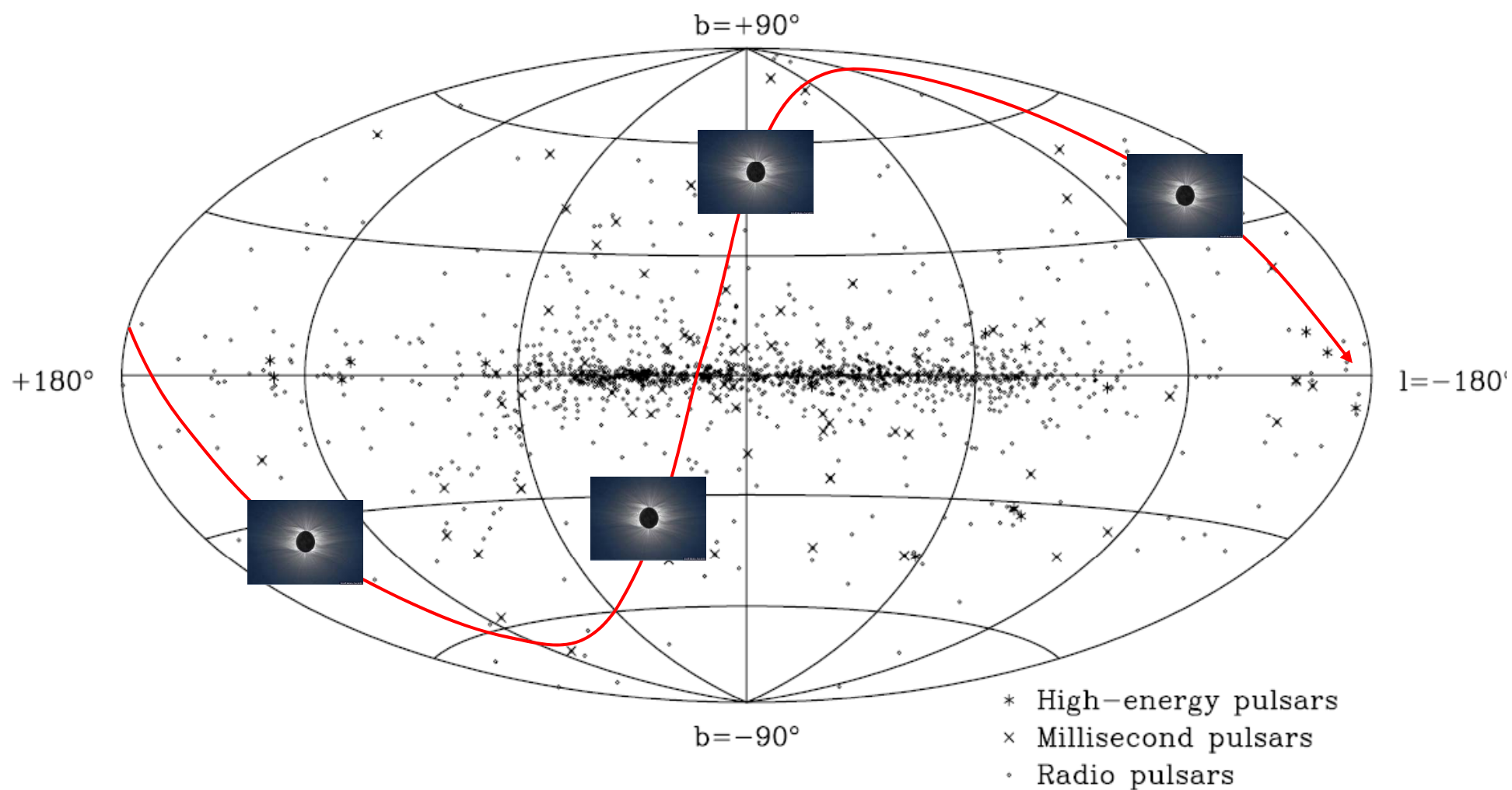


FIG. 3.—Distribution of pulsars on a Hammer-Aitoff equal-area projection in Galactic coordinates with the Galactic center at the center of the plot.



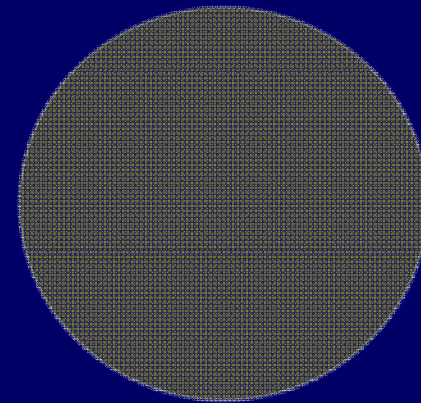
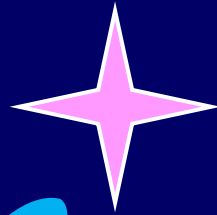
Pulsar RM Coronal Mag. Fields.

Strongly polarised &

“Pulsating” = FM

(Freq. modulation)

1-1000 x few % Jy



20,000-20,000 Jy



The Magnetic Field of the Solar Corona from
Pulsar Observations

ORD, JOHNSTON AND SARKISSIAN

Table I. Possible Targets

Pulsar Name	Ecliptic Longitude : Latitude	Flux (mJy) at 1400 MHz
J1652-2404	254.73 : -1.50	1.1 ^a
J1721-2457	261.18 : -1.81	unknown
J1730-2304	263.19 : 0.19	4 ^b
J1733-2228	263.86 : 0.821	2.3 ^d
J1753-2501	268.52 : -1.576	2.3 ^d
J1756-2251	269.26 : 0.57	0.6 ^e
J1756-2435	269.30 : -1.1554	2.0 ^d
J1757-2421	269.42 : -0.9307	3.9 ^d
J1757-2223	269.50 : 1.04	1.1 ^c
J1759-2205	269.86 : 1.3467	1.3 ^d
J1759-2302	269.96 : 0.40	1.3 ^c
J1801-2304	270.31 : 0.36	2.2 ^d
J1803-2137	270.89 : 1.8282	7.6 ^d
J1807-2459A	271.66 : -1.57	1.1 ^d
J1817-2311	273.91 : 0.20	unknown
J1822-2256	275.28 : 0.392	2.4 ^d
J2048-1616	310.12 : 1.49	13 ^a

$$n(r, \theta, \phi) = n_{CH}(r) + [n_{CS}(r) - n_{CH}(r)] \times \exp[-\theta^2/w^2(r, \phi)]. \quad (10)$$

Where,

$$n_{CH}(r) = \left[16.15 \left(\frac{r}{R_{\odot}} \right)^{-4.39} + 9.975 \left(\frac{r}{R_{\odot}} \right)^{-4.09} + 1.099 \left(\frac{r}{R_{\odot}} \right)^{-2} \right] \times 10^5. \quad (11)$$

and the streamer (n_{CS}) is given by:

$$n_{CS}(r) = \left[365 \left(\frac{r}{R_{\odot}} \right)^{-4.31} + 3.6 \left(\frac{r}{R_{\odot}} \right)^{-2} \right] \times 10^5, \quad (12)$$

$$B_r = \sum_{lm} P_l^m(\cos \theta) (g_{lm} \cos m\theta + h_{lm} \sin m\theta) \times \left((l+1) \left(\frac{R_{\odot}}{r} \right)^{l+2} - l \left(\frac{r}{R_s} \right)^{l-1} c_l \right) \quad (6)$$

$$B_{\theta} = -1 \times \sum_{lm} \left(\left(\frac{R_{\odot}}{r} \right)^{l+2} + \left(\frac{r}{R_s} \right)^{l-1} c_l \right) \times (g_{lm} \cos m\theta + h_{lm} \sin m\theta) \frac{\delta P_l^m(\cos \theta)}{\delta \theta} \quad (7)$$

$$B_{\phi} = \sum_{lm} \left(\left(\frac{R_{\odot}}{r} \right)^{l+2} + \left(\frac{r}{R_s} \right)^{l-1} c_l \right) \frac{m}{\sin \theta} \times (\cos \theta) (g_{lm} \sin m\theta - h_{lm} \cos m\theta) P_l^m(\cos \theta) \quad (8)$$

$$c_l = -\frac{R_{\odot}}{R_s}, \quad (9)$$

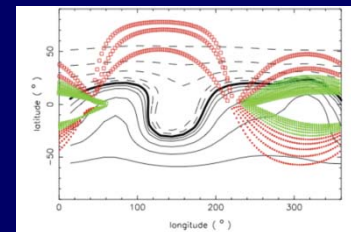


Figure 1. The radial component of the magnetic field of the sun at a distance of 2.5 solar radii.

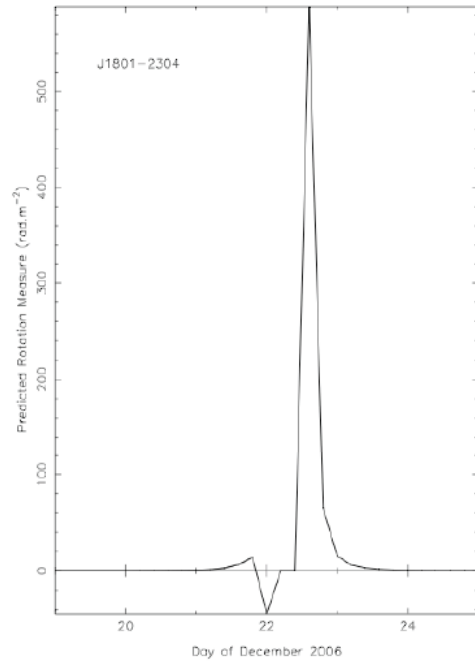


Figure 2. The predicted excess Faraday rotation for J1801-2304. The pulsar was observed throughout this period, unfortunately the observation at the height of the predicted Faraday rotation has insufficient signal to noise ratio to allow a confirmation

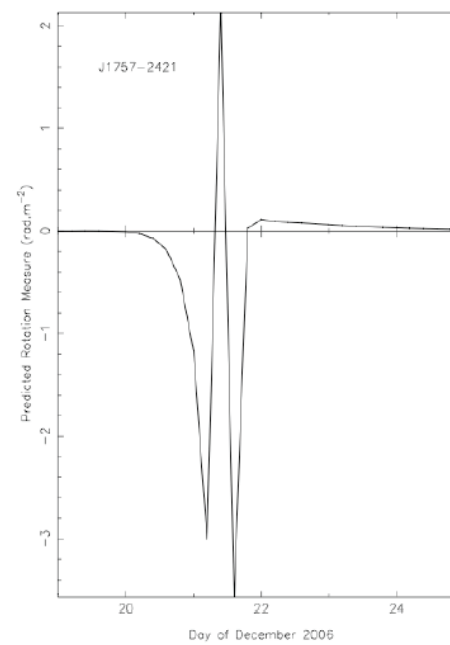


Figure 3. The predicted excess Faraday rotation for J1757-2421. The line of sight to this pulsar traverses regions of the corona that are symmetric in their magnetic field and electron properties, therefore it displays little net Faraday rotation.

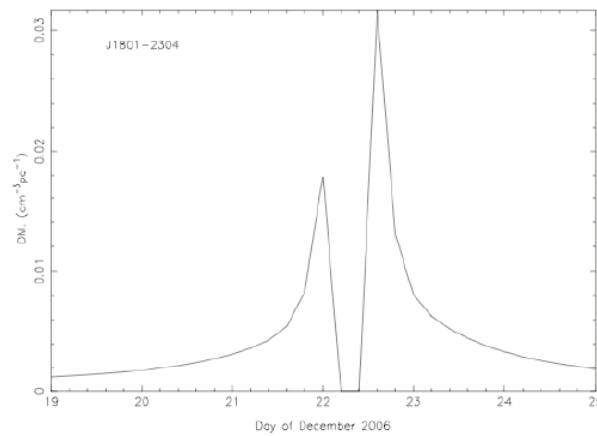
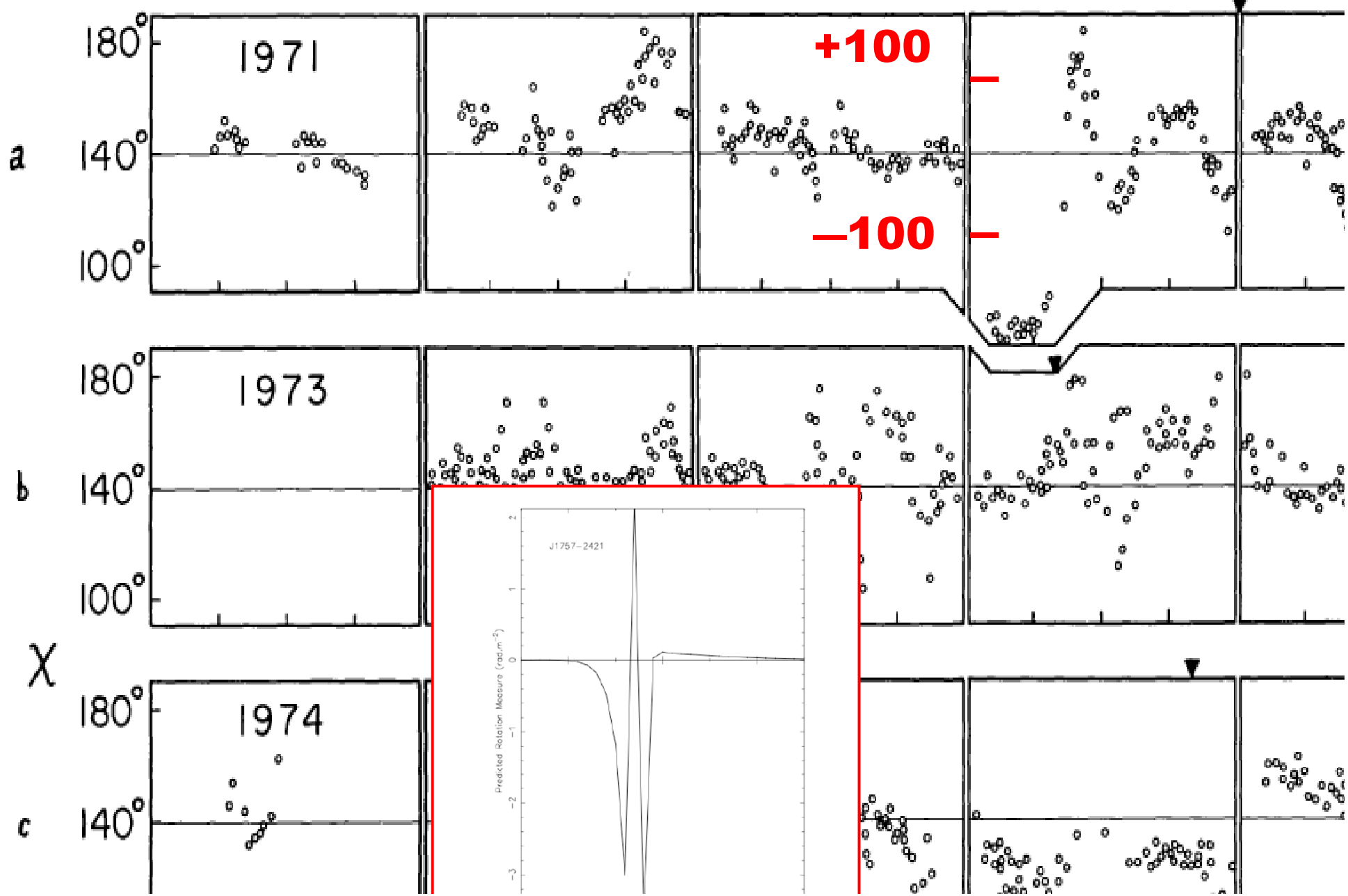


Figure 4. The expected DM variations for J1801-2304.



RM



ATNF Pulsar Catalogue



[Catalogue Tutorial](#) | [Documentation](#) | [Expert](#) | [ATNF Pulsar Home](#) | [Pulsar Tutorial](#) | [Glitch table](#) | [Feedback](#) | [Download](#) | [History](#)

Catalogue version: 1.47

TABLE

PLOT

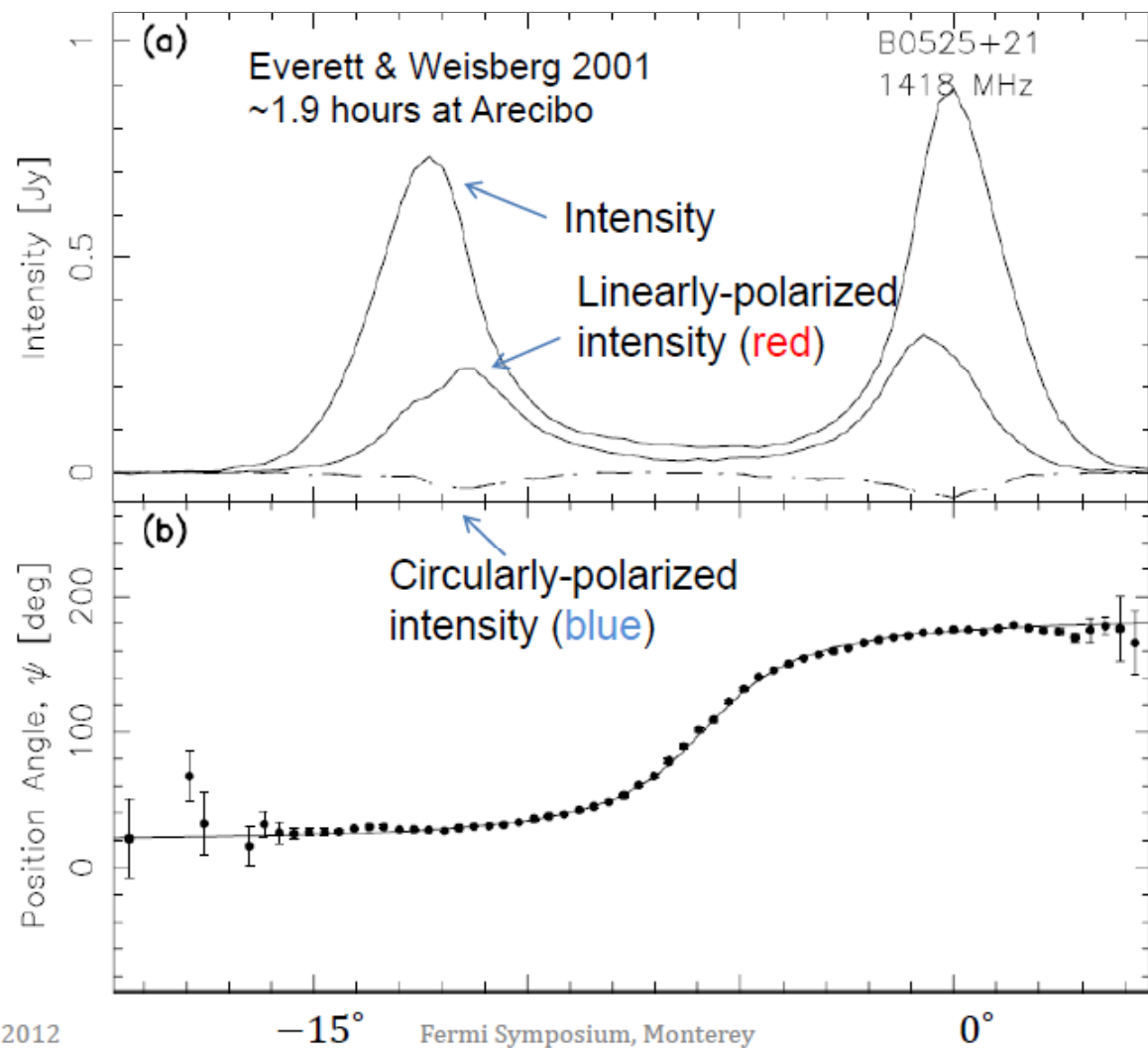
Clear Parameters

Clear Conditions

Clear All

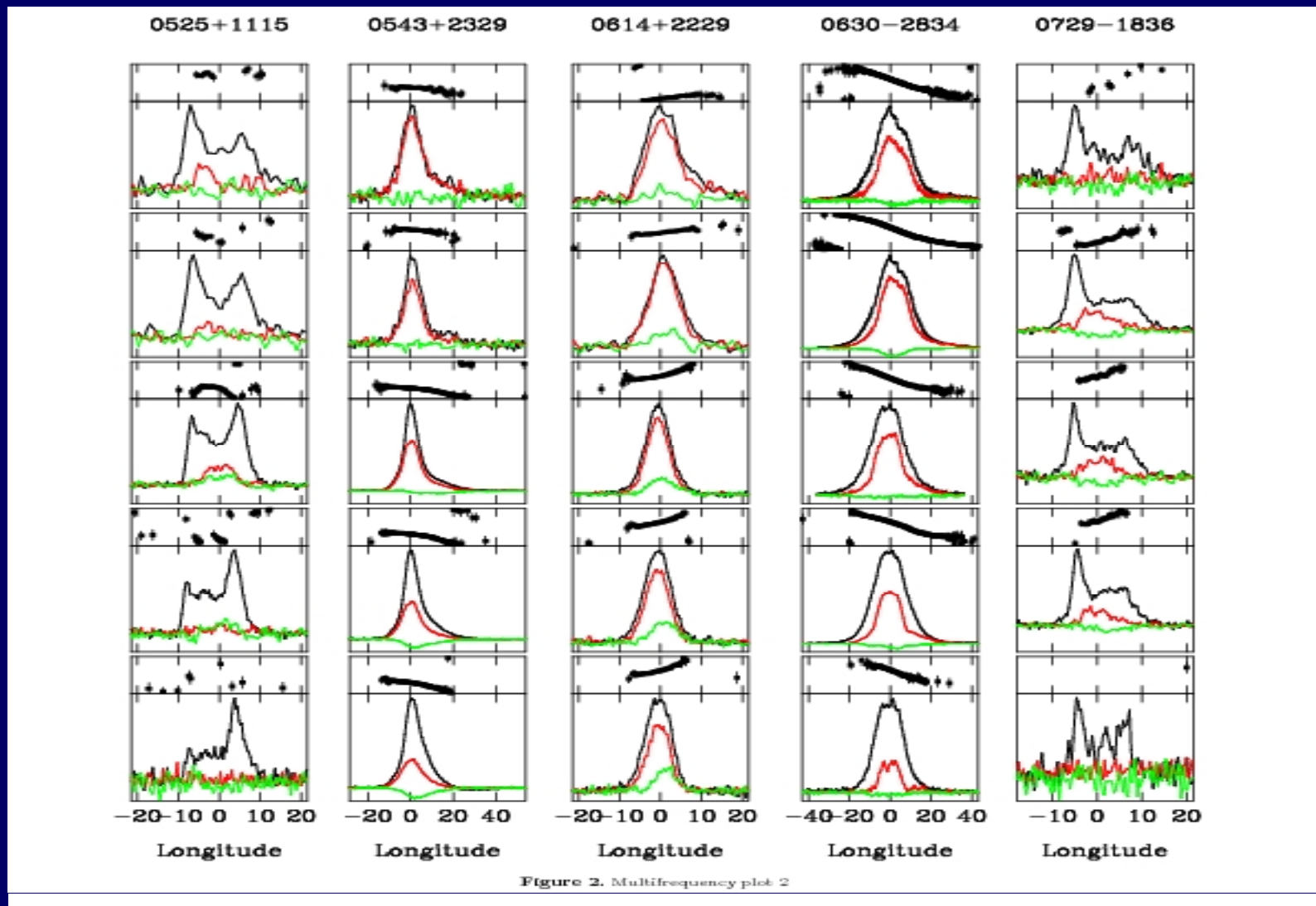
[Display parameters](#) **Predefined Variables**

<input type="checkbox"/> Name	<input type="checkbox"/> JName	<input checked="" type="checkbox"/> RaJ	<input checked="" type="checkbox"/> DecJ	<input type="checkbox"/> PMRA	<input type="checkbox"/> PMDec
<input type="checkbox"/> PX	<input type="checkbox"/> PosEpoch	<input type="checkbox"/> ELong	<input type="checkbox"/> ELat	<input type="checkbox"/> PMELong	<input type="checkbox"/> PMELat
<input type="checkbox"/> GL	<input type="checkbox"/> GB	<input type="checkbox"/> RaJD	<input type="checkbox"/> DecJD		

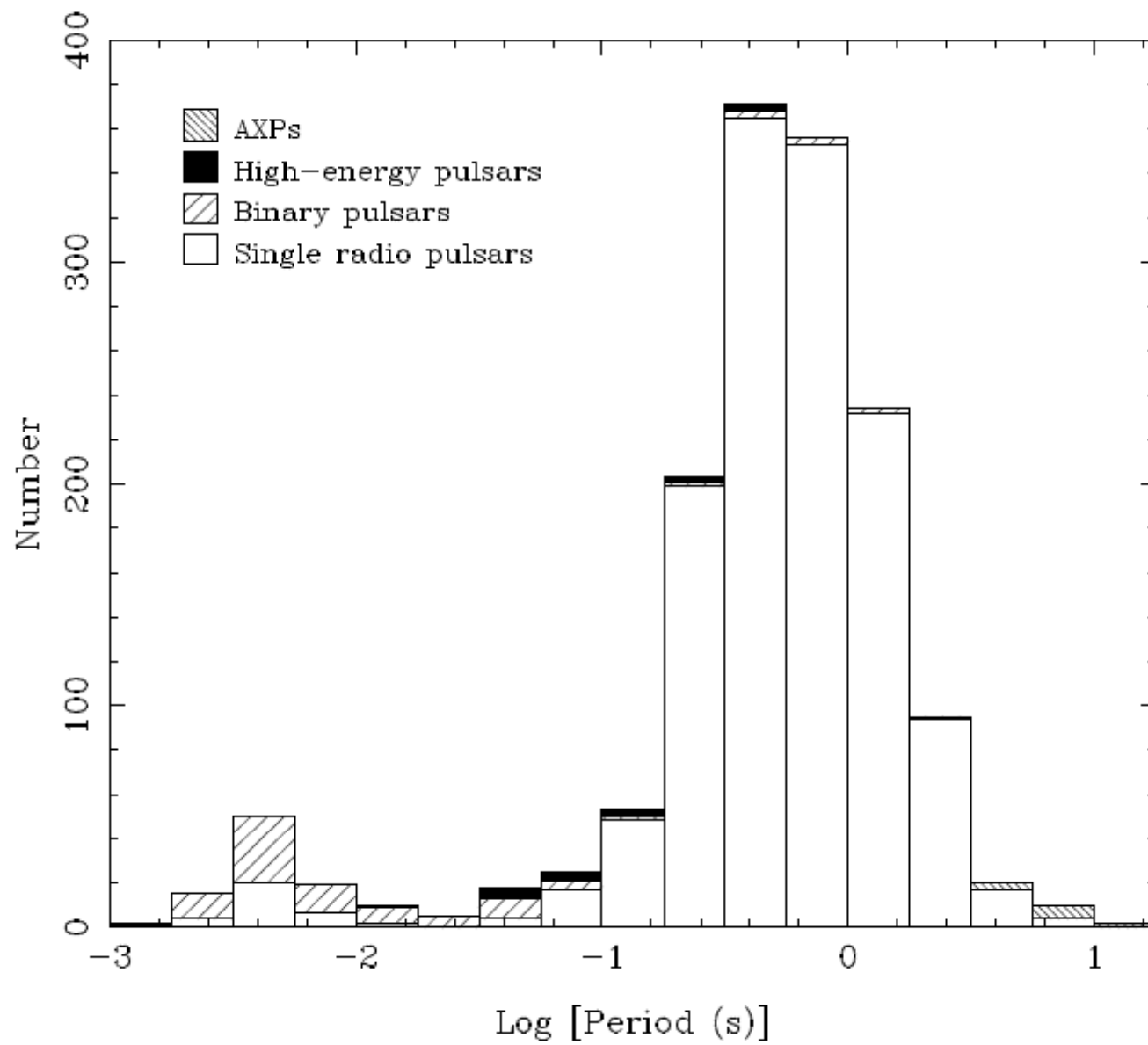


October 2012

GMRT – Parkes, Pulsar Polarization survey: 243, 325, 660, 1400, 3100 MHz

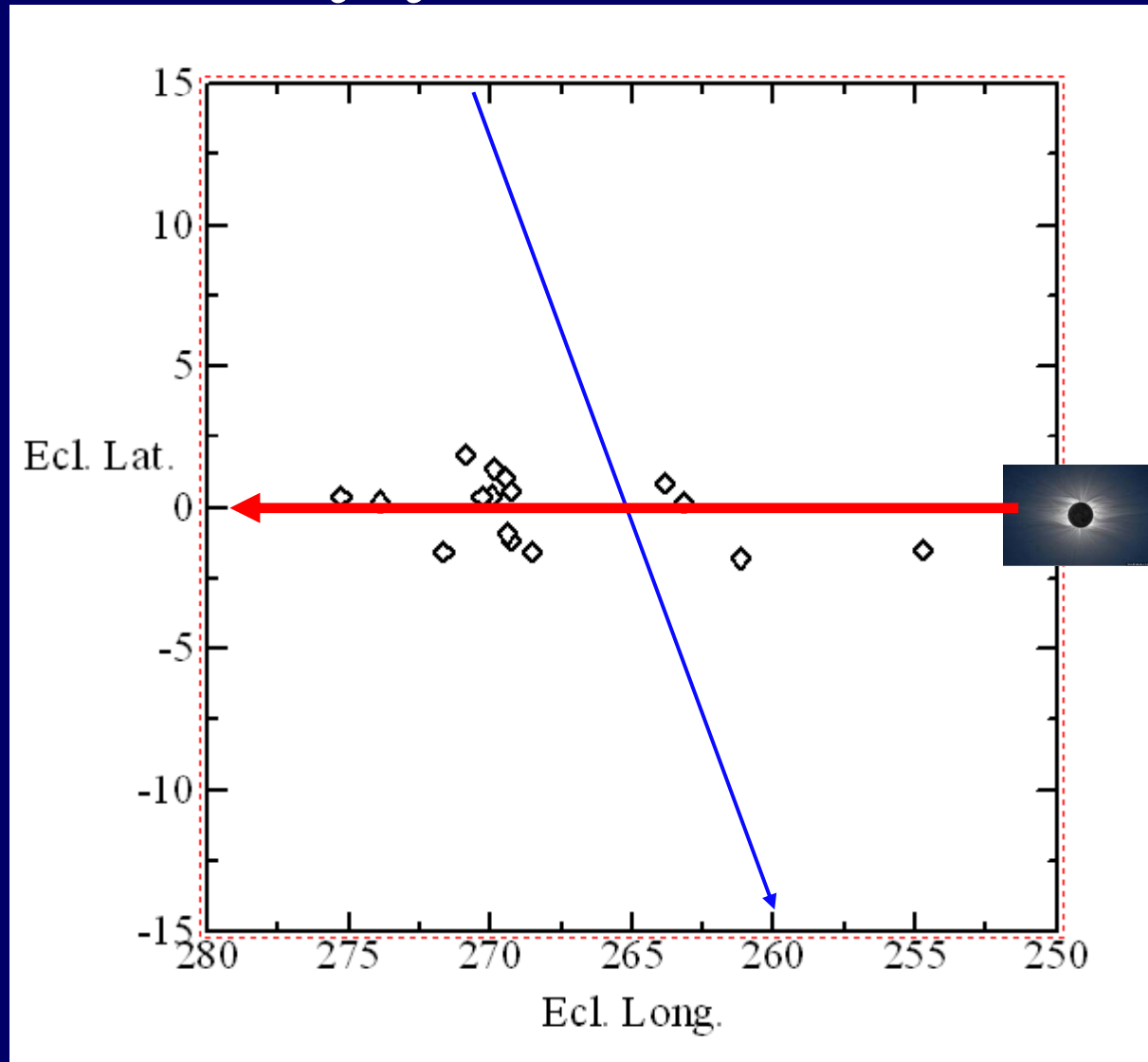


Johnston, Karasterigiou, Mitra, Gupta (2008)

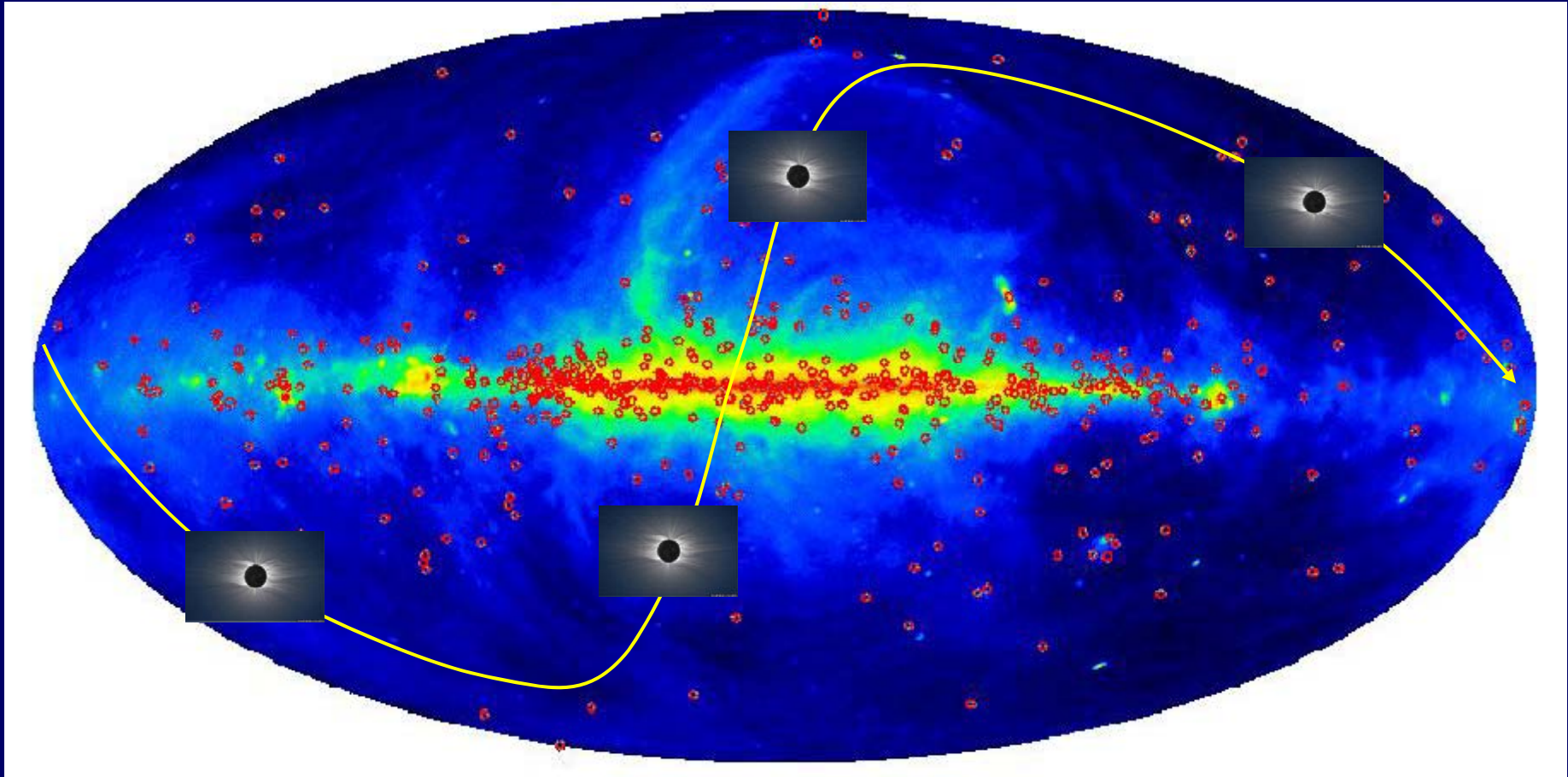


Ecliptic plane & Pulsars

December every year



Ecliptic plane & Pulsars



Toward SKA

ABOUT LOFAR

- * General information
- * System
- * News Archive
- * Informatie over LOFAR (in Dutch!)



[Image Gallery](#)

Address

Oude Hoogeveensedijk 4
7991 PD Dwingeloo
The Netherlands

(+31) (0)521 595 10

Contact us

ASTRON

Initiator: ASTRON
Netherlands Institute for
Radio Astronomy



This project was co-financed by the EU, the European Fund for Regional Development and the Northern Netherlands Provinces (SNN), and EZ/KOMPAS.

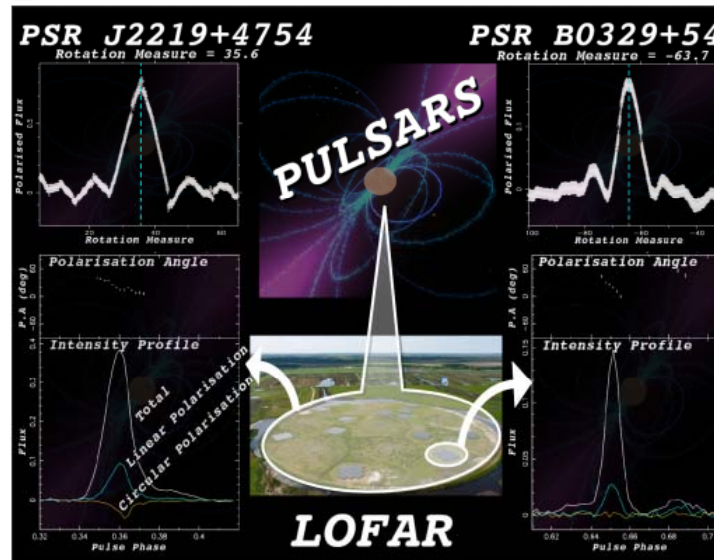
* About LOFAR * News Archive

First Pulsar Polarisation Profiles with LOFAR

* 12 May 2012: Open Day at LOFAR

telescope

Wed, 16/02/2011 - 00:00



Copyright: ASTRON

The image shows two of the very first polarisation profiles of pulsars observed with the LOFAR HBAs, those of PSR B0329+54 and PSR J2219+4754 (lower panels). It is the first time that such high-quality polarisation information is recorded at these frequencies by coherently combining the complex voltages from several LOFAR sub-stations. Although the polarisation profiles are not yet calibrated, work is being done in order to correct for the geometric and instrumental effects that affect the polarisation measurements during observation.

Observing pulsar polarisation at low frequencies can give insight into the magnetospheric physics of pulsars. The properties of polarised pulsar emission can be combined with those



[Informatie over LOFAR in het Nederlands](#)

ASTRON initiated LOFAR as a new and innovative effort to force a breakthrough in sensitivity for astronomical observations at radio-frequencies below 250 MHz.